Understanding the multi-scale structure and digestibility of different waxy maize starches

Jinchuan Xu, Ling Chen, Xinbo Guo, Yi Liang, Fengwei Xie

PII: S0141-8130(19)36804-7

DOI: https://doi.org/10.1016/j.ijbiomac.2019.12.110

Reference: BIOMAC 14137

To appear in: *International Journal of Biological Macromolecules*

Received date: 25 August 2019

Revised date: 28 November 2019

Accepted date: 14 December 2019

Please cite this article as: J. Xu, L. Chen, X. Guo, et al., Understanding the multi-scale structure and digestibility of different waxy maize starches, *International Journal of Biological Macromolecules*(2019), https://doi.org/10.1016/j.ijbiomac.2019.12.110

Understanding the multi-scale structure and digestibility of different waxy maize starches

Jinchuan Xu [a], Ling Chen [a, **], Xinbo Guo [a], Yi Liang [d], Fengwei Xie [b,c, *]

[a] *Ministry of Education Engineering Research Center of Starch & Protein Processing, Guangdong Province Key Laboratory for Green Processing of Natural Products and Product Safety, School of Food Science and Engineering, South China University of Technology, Guangzhou, Guangdong, 510640, China*

[b] *International Institute for Nanocomposites Manufacturing (IINM), WMG, University of Warwick, Coventry CV4 7AL, United Kingdom*

[c] *School of Chemical Engineering, The University of Queensland, Brisbane, Qld 4072, Australia*

[d] *Guangdong Zhongqing Font Biochemical Science and Technology Co. Ltd., Maoming, Guangdong 525427, China*

Corresponding authors:

****** felchen@scut.edu.cn (L. Chen)

* d.xie.2@warwick.ac.uk, fwhsieh@gmail.com (F. Xie).

Abstract: This work concerns different cultivars of waxy maize starch (WMS), from which a significant correlation between the multi-scale structure and the digestibility has been identified. WMSs show a typical A-type crystalline polymorph. The surface porosity of WMS granules facilitates their digestibility. In contrast, the *in vitro* digestion results indicate that the resistant starch (RS) content increased with higher contents of amylose, single helices, and surface short-range ordered structures. Resistant starch (RS) was found to be made up of single helices and perfect crystallites formed by the fraction of chains with a degree of polymerization (DP) between 13 and 24. Slowly digestible starch (SDS) consists of single helices. Rapidly digestible starch (RDS) is mainly composed of disordered molecular chains in the amorphous regions of starch. This work reveals the relationship between the multiscale structure and digestibility of different WMSs and can provide guidance for the application of WMSs in food or non-food fields.

Keywords: waxy maize starch; multi-scale structure; digestibility; correlation analysis

1. Instruction

Starch is one of the most important ingredients in foods and the most important source of energy for human beings [1]. Starch is cheap, renewable, biodegradable, environmentally friendly, and nutritious [2]. Generally, native starches comprise 20–30% linear amylose and 70–80 % highly-branched amylopectin [3], whilst waxy starches consist of mostly amylopectin [4]. Waxy starches have greater paste viscosities and a lower tendency to retrogradation [5], being advantageous for applications. Waxy maize is generally contained in fresh foods such as canned or frozen maize kernels [6].

Starch granules are biosynthesized in higher plants with a highly sophisticated supramolecular structure containing clusters, helices, and crystallites [7]. The size and shape of starch granules also depend on the starch variety. For example, compare to regular wheat starch, waxy wheat starch has more spherical disc-like granules [8], smaller average granule diameters, and a higher degree of crystallinity [9]. How the multiscale starch structure determines the properties of starch is scientifically interesting and practically important.

The digestibility of starch can be influenced by the granule, crystalline and molecular structures [10, 11]. According to *in vitro* digestion analysis, starch can be typically classified into three major fractions: rapidly digestible starch (RDS), slowly digestible starch (SDS), and resistant starch (RS) [12]. Both RS and SDS are found to present health benefits. RS can improve the lipid and cholesterol metabolisms, have prebiotic effects on colon microorganisms, and reduce the risks of ulcerative colitis and colon cancer [13]. SDS can give a lower glycemic response, higher glucose tolerance, and lower the blood lipid level [14].

A previous study [5] showed that waxy rice and waxy tapioca starches had less retrogradation tendency, which was related to the higher proportion of chains with DP 6–11 and the lower proportion of chains with DP 12–24. For waxy maize starch, Zhang et al. [15] found the action of either the 0.1% (w/v) or 0.5% (w/v) alkaline solution occurs at the smaller length-scale (i.e., double

helices and crystallites), which causes changes to the starch digestion behavior [16], whereas the large-scale structural motifs such as lamellae, growth rings and blocklets were largely conserved. Starches from different waxy wheat varieties were shown to have similar granule morphology, average granule size, crystalline structure, long-range and short-range ordered structures, swelling power, gelatinization properties, and *in vitro* digestibility [9]. For waxy maize starch (WMS), debranching for a longer time and a higher degree of recrystallization could lead to a higher RS content [17]. However, there has been no systematic study regarding the relationship between the multi-scale structure and digestibility of different cultivars of WMS.

In this work, five WMS cultivars were selected as the model materials to compare their granule morphology, degree of crystallinity, degree of debranching, short-range molecular orders, helical conformations, and amylopectin chain length distribution. Based on that, the relationship between the multi-scale structures and digestibility was then established. The results from the present study are crucial for the rational development of starch-based food and non-food products.

2. Materials and methods

2.1. Materials

Five waxy maize cultivars (L1, L2, L3, L4, and L5) were kindly supplied by the Guangdong Academy of Agricultural Sciences, which was a line developed by inbreeding. Starch was extracted from waxy maize according to a previous study [18] and the samples were coded as L1, L2, L3, L4, and L5, respectively.

Porcine pancreatic α-amylase (P-7545, 8×USP/g) and amyloglucosidase (A3306, 318 U/mL) were purchased from Sigma-Aldrich (USA). All other chemicals (reagent grade) were supplied by Nanjing Chemical Reagents Co., Ltd. (China).

2.2. Chemical analysis of starch

The protein and lipid contents of the starch samples were determined according to the Standard AOAC methods 979.09 and 948.15, respectively [19]. The ash was determined by the AOAC standard method 942.05 [19]. The moisture content (MC) of each starch was determined using a moisture analyzer (MA35, Sartorius Stedim Biotech GmbH, Germany). The chemical composition of different WMSs was shown in Table 1.

The apparent amylose content (AAC) of starch was determined by the AACC method, which was calculated based on a standard curve.

The *in vitro* digestibility of starch was determined using a modified method of Englyst [20]. In brief, 1 g of starch (dry-based) was dispersed in 20 mL of 0.1 M sodium acetate buffer (pH = 5.2) and hydrolyzed with the enzyme mixture. Then, the glucose content was determined by a glucose oxidase-peroxidase (GOPOD) assay kit (K-GLUC) (Megazyme, Ireland) [21]. Each test was analyzed in triplicate.

2.3. Structural characterization of starch

The particle size of starch was performed using a laser-diffraction analyzer (Malvern Mastersizer 2000, UK) with a flow-through reservoir (1000 mL). The starch samples were loaded into the reservoir until completely dispersed in anhydrous ethanol. The obscuration value was then adjusted to be between 12 % and 17 %. The refractive indices of starch samples and the dispersing reagent ethanol was 1.54 and 1.36, respectively. All the measurements were analyzed in replicate.

The morphology of starch granules was observed using a scanning electron microscope (ZEISS EVO18, Germany). The samples were mounted on an aluminum platform and coated with gold using a 108-auto sputter coater (Cressington Scientific Instruments Ltd, UK).

The fractal structures of starch were investigated using a small-angle X-ray scattering (SAXS) system (Anton-Paar, Austria) following our previously established conditions (Cu-Kα radiation

source, 50 mA, 40 kV, and 0.1542 nm wavelength) [22]. All data were analyzed using SAXSquant 3.0 software.

The crystallinity of starch was measured using an Xpert PRO diffractometer (PANalytical, Netherlands) with Cu-Kα radiation at 40 mA and 40 kV. The diffraction scanning was recorded from 5° to 35° at a speed of 10°/min and a step size of 0.033°. Relative crystallinity (RC) was measured based on the ratio of the diffraction peak areas to the total diffractogram area [23]. Each test was performed in triplicate.

The weight-average molecular weight (M_w) and the mean square radius of gyration (R_g) of starch were analyzed using a GPC (Waters, USA) system equipped with a MALS detector (Wyatt, USA), according to our previous procedure [24]. The data were analyzed using ASTRA V (Ver. 5.3.4.20) software. All samples were tested in triplicate.

The chain length distribution of amylopectin that extracted from starch was analyzed using a high-performance anion-exchange chromatography (HPAEC) system with the detailed method was described previously [18]. All samples were tested in duplicate.

Solid-state ^{13}C cross-polarized magic-angle spinning nuclear magnetic resonance (CP/MAS NMR) was performed on a Bruker AVANCE III HD 400 spectrometer (Bruker, Germany) following our previous procedure and conditions (100.613 MHz and 295 K) [24]. Over 6000 scans were recorded for a spectrum with a recycle delay of 2 s. The spectra were analyzed using PeakFit v4.12 software.

The molecular interactions of starch were analyzed using an attenuated total reflectance Fourier-transform infrared (ATR-FTIR) spectrometer (Bruker, Germany) with a DTGS (deuterated triglycine sulfate) detector. For each sample, 64 scans were collected in the wavenumber range of 4000–400 cm^{-1} at a resolution of 4 cm^{-1}. The air was taken as the background. Three replicated measurements were recorded for each sample.

2.4. Statistical analysis

The data were analyzed using the SPSS 22.0 statistical software. Analysis of variance (ANOVA) was carried out followed by Duncan's multiple-range test. The significance level was set at $p < 0.05$.

3. Results and discussion

3.1. AAC and *in vitro* digestibility

Maize starch consists of amylose and amylopectin, and amylose is one of the major factors affecting the physicochemical properties of starch. Moreover, the amylose/amylopectin ratio determines the granule size, multi-scale structure and functional properties of starch. The AAC of starch samples vary between 1.8 and 12.5 % and is in the sequence of L1 > L3 > L2 ≈ L4 ≈ L5 (Table 2). L1 has the highest AAC (12.5%), which is still lower than that of normal maize starch (around 25 %) [25-27]. With a higher amylose content, the resistant starch (RS) content increases whereas the rapidly digestible starch (RDS) content decreases. Regarding this, RS could be mainly composed of amylose, which is more resistant to digestive enzymes, whereas amylopectin contributes to RDS. Overall, WMSs have higher digestibility (RDS+SDS content over 80 %).

3.2. Granule size distribution and granule morphology

The three size groups of starch granules can be distinctly divided: type A (> 15.9 μm), type B (5.3–15.9 μm), type C (< 5.3 μm) [28]. Type A granules begin to form the initial flower (grain begin to grow) and continue to grow throughout the grain growth period. Type B and C granules are supposed to be initiated at a specific time point in the later flower period depending on the cultivar, location, and extracted method [29]. The granule size distributions of different WMSs are illustrated in Fig. 1. It can be seen that all the samples have two populations of particles. The major group of particles have sizes between 5–13 μm whilst the other group of particles are smaller (0.3–3 μm). Given this, the WMSs have two types of starch granules, type B and type C, with type B granules

being the dominant type. Compared with the other samples, L2 and L4 present slightly higher median diameters (D_{50}) (Table 2), but lower peaks (Fig. 1).

Fig. 2 shows the SEM images of different WMSs. Most of the starch granules are over 5 μm, and a small portion of them are smaller than 3 μm, which corresponds to the granule size distribution results. In addition, WMS granules have a spherical, ellipsoidal, square or irregular shape, and the surface of most granules is smooth, which is similar to a previous study [30]. Compared with L3 (4.9% AAC) and L4 (2.2% AAC), L2 (3.1% AAC) has a higher RDS content, which means L2 can be easily hydrolyzed by digestive enzymes. This coincides with the granule surface of L2 presenting holes, which allows easier entrance of enzymes into the core of the granule. In addition, the surface of some granules of L3 shows some indents, which may be caused by an incomplete development during the growth period. While these WMSs show similar granule sizes, the surface structure of starch granules (such as pores) is significantly correlated with digestibility.

3.3. Molecular weight and its distribution

Table 3 shows the M_w, R_g, and molecular mass distribution of different WMSs. The M_w values follows the order of L5 > L4 > L3 > L2 > L1. The R_g of WMSs increase with higher M_w, except for L1. For L1, amylose molecules could intertwine with amylopectin molecules forming larger space between chains during the growth of starch granules, which results in higher R_g. In addition, M_w increases with increasing amylopectin content, which is as expected since amylopectin has much large M_w than amylose. A higher amylopectin content also leads to a gradual increase in the M_w distribution. For example, for L1, 87.33% of the molecules have M_w lower than 5×10^6, whilst 100 % of L5 molecules distribute in the range over 3×10^7. These results show significant differences in M_w distribution among WMSs.

3.4. Chain-length profiles of amylopectin

Table 3 shows the chain length distribution of the branched amylopectin, which can be divided into four parts [31, 32]: f_a (DP 6–12), f_{b1} (DP 13–24), f_{b2} (DP 25–36), and f_{b3} (DP >36).

There is no significant difference in the chain length of DP 6–12 among different WMSs, indicating that f_a chains were generated by similar starch synthases during growth. For all WMSs, f_{b1} shows the highest content (over 41 %) compared other fractions of chains. Thus, f_{b1} chains may have a major effect on the properties and functions of starch. The content of f_{b2} decreases with increasing amylopectin content.

3.5. Helical structure

Nuclear magnetic resonance spectroscopy (NMR) was used to characterize the changes of helical structures of WMSs and the results are shown in Fig. 3. The signal between 95–105 ppm can be attributed to the chemical shift of C_1 of starch; that at 81 ppm can be ascribed to C_4; that between 68–78 ppm should be assigned to $C_{2,3,5}$; and that at 62 ppm can be linked to C_6. The chemical shifts at around 102 and 103 ppm of C_1 are typically considered to be due to the V-type single helix (SH) [33]; 103 ppm is also related to the junction points between amorphous starch (AS) and amylopectin double helix (DH) [24]. The chemical shifts at 101.5, 100.5 and 99.4 ppm in the C_1 region are typically identified as the A-type double helix [33, 34]. Thus, these peaks can be used to characterize the short-range ordered structure of starch. The NMR spectrum of a starch sample can be subtracted by the amorphous to obtain SH and DH contents using the intensity at 84 ppm as a reference [24]. The contents of DH in WMSs are in the range of 30.7–34.9%, the SH contents are between 0 and 3.31%, and those of AS are between 61.8 and 67.7% (Table 5). The RDS of WMS increases with higher amounts of AS. This indicates that the molecular chains in the amorphous regions of starch can be more easily digested, which contributes to RDS. With increasing content of SH, the RDS content of WMS decreases, whereas the SDS and RS contents increase. This indicates that SH is an important component of SDS and RS.

3.6. Crystalline structure

The crystallinity of starch is an important parameter to characterize the physicochemical properties (e.g., digestibility) of starch [35]. Depending on the arrangement of DH or SH by short

amylopectin chains or amylose, the crystalline structure of starch can be defined as A, B, C, or V [36, 37]. As shown in Fig. 4, WMSs display a typical A-type crystalline polymorph with main diffraction peaks at around 15°, 17°, 18° and 23° (2θ), with 17° and 18° forming a doublet. There is no significant diffraction peak at 20° 2θ due to the low amylose content. The crystallinity of WMSs follows the order L5 ≈ L4 ≈ L2 ≈ L3 > L1, indicating that the crystallinity increases slightly with increasing amylopectin content in WMS (Table 2 and Table 5). Interestingly, the RS content decreases with increasing crystallinity. Given this, RS could be mainly contributed by amylose.

3.7. Surface short-range order structure

The FTIR spectrum in the region of 800–1200 cm^{-1} is normally considered to be sensitive to the oscillation frequency of starch chemical bonds. Specifically, the absorbance band at 1045 cm^{-1} is related to the crystalline structure; and the band at 1022 cm^{-1} can be linked to AS, and the band at 995 cm^{-1} can be related to the intramolecular hydrogen bonding of the hydroxyl group at C-6 [38-40]. Furthermore, the ratio of intensity at 1045/1022 cm^{-1} ($R_{1045/1022}$) can be used to characterize the changes in the starch crystalline structure [22, 41]. Fig. 5 shows the ATR-FTIR spectra of different WMSs, with their $R_{1045/1022}$ values listed in Table 4. All WMSs, except for L1, do not show a significant difference in the surface short-range ordered structure. However, a higher content of the short-range ordered structure ($R_{1045/1022}$) coincides with a higher RS content. This indicates that the surface short-range ordered structure of starch might provide a resistant effect against digestive enzymes.

3.8. Lamellar structures

From Fig. 6, it can be seen that the position of the peak is at around 0.7 nm^{-1}, which corresponds to the 9-nm semi-crystalline structure based on the Woolf-Bragg's equation $D = 2\pi/q$ [42]. The values of D are in the sequence of L1 > L3 > L2 = L4 > L5 (Table 6). For different WMSs, there is a significant difference in D, which increases with increasing amylose content. L1 has the

highest D (90.61 Å), which could be related to its highest double-helical structure and $R_{1045/1022}$ value (Table 5).

3.9. Structure-digestibility relationship

The relationship between the multi-scale structure and digestibility of WMS was investigated by Pearson correlation analysis, including RC, D_{50}, $R_{1045/1022}$, DH content, SH content, AS content, chain length distribution of debranched amylopectin, M_w, R_g, scattering vector (q_{peak}), D, AAC, RDS, SDS, and RS. Table 7 shows that there are significant correlations between the multi-scale structure and digestibility of WMS. Specifically, RDS is strongly correlated with f_{b2} (r = 0.862, p < 0.01), M_w (r = 0.845, p < 0.01), q_{peak} (r = 0.669, p < 0.05), AS (r = 0.647, p < 0.05) and RC (r = 0.772, p < 0.01), indicating that RDS is most likely to be composed of disordered molecular chains in the amorphous regions of starch. RDS has a negative correlation with AAC (r = −0.696, p < 0.05), D (r = −0.666, p < 0.05), SH (r = −0.887, p < 0.01), AS (r = −0.647, p < 0.05), and $R_{1045/1022}$ (r = −0.678, p < 0.05), suggesting that the more ordered structure is formed by amylose, resulting in a lower RDS. SDS is positively correlated with SH (r = 0.723, p < 0.05), showing that SDS is mainly composed of SH. SDS is negatively correlated with M_w (r = −0.715, p < 0.05), meaning that a higher M_w contributes to a lower SDS content. RS has a positive correlation with AAC (r = 0.872, p < 0.01), f_a (r = 0.642, p < 0.05), f_{b1} (r = 0.746, p < 0.05), D (r = 0.742, p < 0.05), SH (r = 0.974, p < 0.01), and $R_{1045/1022}$ (r = 0.803, p < 0.01), indicating that RS is mainly composed of SH structure formed by amylose and f_a and f_{b1} chains. RS has a significant negative correlation with f_{b3} (r = −0.741, p < 0.05), M_w (r = −0.881, p < 0.01), q_{peak} (r = −0.742, p < 0.05), AS (r = −0.755, p < 0.05), and RC (r = −0.931, p < 0.01), which implies that larger M_w leads to a higher AS content and a higher RC, resulting in a lower RS content.

4. Conclusions

In this work, a significant correlation between the multi-scale structure and digestibility of WMSs has been established. On the one hand, enzymatic hydrolysis can occur by contact with AS formed by disordered starch molecular chains. RDS was found to be mainly composed of disordered starch molecular chains as the RDS content is positively correlated with f_{b2} (DP 25–36) chains, M_w, AS content, and RC. On the other hand, enzymes can only hydrolyze part of the order molecular chains located in the crystalline regions of starch. The relatively perfect crystalline structure will inhibit the hydrolysis by digestive enzymes. SDS is positively correlated with SH content and AS content. This indicates that SDS is mainly composed of ordered molecular structures such as SH (0.723^{**}). Moreover, there is a positive correlation between RS and AAC, f_a (DP 6–2) and f_{b1} (DP 13–24), D, SH content and $R_{1045/1022}$. This suggests that the ordered structure arranged by SH and the compact short-range ordered structure formed by short chains has a major contribution to the digestion resistance of starch. This study improves our understanding of the relationship between the multi-scale structure and digestibility of WMS and expands the application of WMS in food or non-food applications.

Acknowledgments

The authors thank for the financial support provided by the National Natural Science Foundation of China (NSFC)–Guangdong Joint Fund under a Key Project (No. U1501214), the National Natural Science Foundation of China (NSFC) under a General Project (No. 31871751), and the Guangdong Provincial Government under a YangFan Innovative and Entrepreneurial Research Team Project (2014YT02S029). F. Xie acknowledges the support from the European Union's Horizon 2020 research and innovation programme under the Marie Skłodowska-Curie grant agreement No. 798225.

References

[1] J. Juansang, C. Puttanlek, V. Rungsardthong, S. Puncha-arnon, D. Uttapap, Effect of gelatinisation on slowly digestible starch and resistant starch of heat-moisture treated and chemically modified canna starches, Food Chemistry, 131 (2012) 500-507.

[2] D. Le Corre, J. Bras, A. Dufresne, Starch nanoparticles: a review, Biomacromolecules, 11 (2010) 1139-1153.

[3] N. Klaochanpong, C. Puttanlek, V. Rungsardthong, S. Puncha-arnon, D. Uttapap, Physicochemical and structural properties of debranched waxy rice, waxy corn and waxy potato starches, Food Hydrocolloids, 45 (2015) 218-226.

[4] B.S. Murray, N. Phisarnchananan, The effect of nanoparticles on the phase separation of waxy corn starch+locust bean gum or guar gum, Food Hydrocolloids, 42 (2014) 92-99.

[5] C. F. Hsieh, W. Liu, J.K. Whaley, Y. C. Shi, Structure and functional properties of waxy starches, Food Hydrocolloids, 94 (2019) 238-254.

[6] D. Ketthaisong, B. Suriharn, R. Tangwongchai, K. Lertrat, Changes in physicochemical properties of waxy corn starches after harvest, and in mechanical properties of fresh cooked kernels during storage, Food Chemistry, 151 (2014) 561-567.

[7] J.F. Robyt, Starch: structure, properties, chemistry, and enzymology, Glycoscience: Chemistry and chemical biology, (2008) 1437-1472.

[8] Z. Zhou, Y. Zhang, X. Chen, M. Zhang, Z. Wang, Multi-scale structural and digestion properties of wheat starches with different amylose contents, International Journal of Food Science & Technology, 49 (2014) 2619-2627.

[9] S. Wang, J. Wang, W. Zhang, C. Li, J. Yu, S. Wang, Molecular order and functional properties of starches from three waxy wheat varieties grown in China, Food Chemistry, 181 (2015) 43-50.

[10] D. Qiao, W. Tu, B. Zhang, R. Wang, N. Li, K. Nishinari, S. Riffat, F. Jiang, Understanding the multi-scale structure and digestion rate of water chestnut starch, Food Hydrocolloids, 91 (2019) 311-318.

[11] N. Li, Z. Cai, Y. Guo, T. Xu, D. Qiao, B. Zhang, S. Zhao, Q. Huang, M. Niu, C. Jia, L. Lin, Q. Lin, Hierarchical structure and slowly digestible features of rice starch following microwave cooking with storage, Food Chemistry, 295 (2019) 475-483.

[12] H.N. Englyst, S. Kingman, J. Cummings, Classification and measurement of nutritionally important starch fractions, European journal of clinical nutrition, 46 (1992) S33-50.

[13] E. Fuentes-Zaragoza, M.J. Riquelme-Navarrete, E. Sánchez-Zapata, J.A. Pérez-Álvarez, Resistant starch as functional ingredient: A review, Food Research International, 43 (2010) 931-942.

[14] M. Miao, T. Zhang, W. Mu, B. Jiang, Effect of controlled gelatinization in excess water on digestibility of waxy maize starch, Food Chemistry, 119 (2010) 41-48.

[15] B. Zhang, E.P. Gilbert, D. Qiao, F. Xie, D.K. Wang, S. Zhao, F. Jiang, A further study on supramolecular structure changes of waxy maize starch subjected to alkaline treatment by extended-q small-angle neutron scattering, Food Hydrocolloids, 95 (2019) 133-142.

[16] D. Qiao, F. Xie, B. Zhang, W. Zou, S. Zhao, M. Niu, R. Lv, Q. Cheng, F. Jiang, J. Zhu, A further understanding of the multi-scale supramolecular structure and digestion rate of waxy starch, Food Hydrocolloids, 65 (2017) 24-34.

[17] L. Cai, Y.-C. Shi, L. Rong, B.S. Hsiao, Debranching and crystallization of waxy maize starch in relation to enzyme digestibility, Carbohydrate Polymers, 81 (2010) 385-393.

[18] J. Xu, Q. Kuang, K. Wang, S. Zhou, S. Wang, X. Liu, S. Wang, Insights into molecular structure and digestion rate of oat starch, Food Chemistry, 220 (2017) 25-30.

[19] A. Intl, Official methods of analysis of AOAC International, Arlington, Va.: AOAC Intl. pv (loose-leaf), (1995).

[20] H.N. Englyst, S.M. Kingman, J.H. Cummings, Classification and measurement of nutritionally important starch fractions, European Journal of Clinical Nutrition, 46 Suppl 2 (1992) S33.

[21] B. McCleary, T. Gibson, V. Solah, D. Mugford, Total starch measurement in cereal products: interlaboratory evaluation of a rapid enzymic test procedure, Cereal Chemistry, 71 (1994) 501-504.

[22] K. Liu, Y. Zu, C. Chi, B. Gu, L. Chen, X. Li, Modulation of the digestibility and multi-scale structure of cassava starch by controlling the cassava growth period, International Journal of Biological Macromolecules, 120 (2018) 346-353.

[23] J. Xu, X. Tan, L. Chen, X. Li, F. Xie, Starch/microcrystalline cellulose hybrid gels as gastric-floating drug delivery systems, Carbohydrate Polymers, 215 (2019) 151-159.

[24] H. Wang, Y. Liu, L. Chen, X. Li, J. Wang, F. Xie, Insights into the multi-scale structure and digestibility of heat-moisture treated rice starch, Food Chemistry, 242 (2018) 323-329.

[25] J. Wang, L. Yu, F. Xie, L. Chen, X. Li, H. Liu, Rheological properties and phase transition of cornstarches with different amylose/amylopectin ratios under shear stress, Starch/Staerke, 62 (2010) 667-675.

[26] X. Liu, L. Yu, F. Xie, M. Li, L. Chen, X. Li, Kinetics and mechanism of thermal decomposition of cornstarches with different amylose/amylopectin ratios, Starch/Staerke, 62 (2010) 139-146.

[27] H. Wang, B. Zhang, L. Chen, X. Li, Understanding the structure and digestibility of heat-moisture treated starch, International Journal of Biological Macromolecules, 88 (2016) 1-8.

[28] D.B. Bechtel, I. Zayas, L. Kaleikau, Y. Pomeranz, Size-distribution of wheat starch granules during endosperm development, Cereal Chemistry, 67 (1990) 59-63.

[29] J.D. Wilson, D.B. Bechtel, T.C. Todd, P.A. Seib, Measurement of Wheat Starch Granule Size Distribution Using Image Analysis and Laser Diffraction Technology, Cereal Chemistry, 83 (2006) 259-268.

[30] P. Chen, L. Yu, L. Chen, X. Li, Morphology and Microstructure of Maize Starches with Different Amylose/Amylopectin Content, Starch/Stärke, 58 (2006) 611-615.

[31] X. Kong, E. Bertoft, J. Bao, H. Corke, Molecular structure of amylopectin from Amaranth starch and its effect on physicochemical properties, International Journal of Biological Macromolecules, 43 (2008) 377-382.

[32] I. Hanashiro, J.-i. Abe, S. Hizukuri, A periodic distribution of the chain length of amylopectin as revealed by high-performance anion-exchange chromatography, Carbohydrate Research, 283 (1996) 151-159.

[33] A. Mihhalevski, I. Heinmaa, R. Traksmaa, T. Pehk, A. Mere, T. Paalme, Structural changes of starch during baking and staling of rye bread, Journal of Agricultural and Food Chemistry, 60 (2012) 8492-8500.

[34] D. Fan, W. Ma, L. Wang, J. Huang, F. Zhang, J. Zhao, H. Zhang, W. Chen, Determining the effects of microwave heating on the ordered structures of rice starch by NMR, Carbohydrate Polymers, 92 (2013) 1395-1401.

[35] N.W.H. Cheetham, L. Tao, Variation in crystalline type with amylose content in maize starch granules: an X-ray powder diffraction study, Carbohydrate Polymers, 36 (1998) 277-284.

[36] J.J.G. van Soest, S.H.D. Hulleman, D. de Wit, J.F.G. Vliegenthart, Crystallinity in starch bioplastics, Industrial Crops and Products, 5 (1996) 11-22.

[37] K. Luengwilai, D.M. Beckles, Structural Investigations and Morphology of Tomato Fruit Starch, Journal of Agricultural and Food Chemistry, 57 (2009) 282-291.

[38] A. Htoon, A.K. Shrestha, B.M. Flanagan, A. Lopez-Rubio, A.R. Bird, E.P. Gilbert, M.J. Gidley, Effects of processing high amylose maize starches under controlled conditions on structural organisation and amylase digestibility, Carbohydrate Polymers, 75 (2009) 236-245.

[39] C. Mutungi, C. Onyango, T. Doert, S. Paasch, S. Thiele, S. Machill, D. Jaros, H. Rohm, Long- and short-range structural changes of recrystallised cassava starch subjected to in vitro digestion, Food Hydrocolloids, 25 (2011) 477-485.

[40] J.J.G. van Soest, H. Tournois, D. de Wit, J.F.G. Vliegenthart, Short-range structure in (partially) crystalline potato starch determined with attenuated total reflectance Fourier-transform IR spectroscopy, Carbohydrate Research, 279 (1995) 201-214.

[41] S. Wang, S. Wang, P. Guo, L. Liu, S. Wang, Multiscale Structural Changes of Wheat and Yam Starches during Cooking and Their Effect on in Vitro Enzymatic Digestibility, Journal of Agricultural and Food Chemistry, 65 (2017) 156-166.

[42] J. Blazek, E.P. Gilbert, Application of small-angle X-ray and neutron scattering techniques to the characterisation of starch structure: A review, Carbohydrate Polymers, 85 (2011) 281-293.

Tables

Table 1. Chemical composition of different WMSs.

Samples	Moisture (%)	Protein (%)	Lipid (%)	Ash (%)
L1	10.6±0.0	0.61±0.12	3.19±0.08	1.39±0.09
L2	10.2±0.4	0.52±0.01	2.13±0.14	1.34±0.12
L3	10.5±0.7	0.56±0.04	2.35±0.16	1.41±0.06
L4	9.8±0.0	0.51±0.02	2.61±0.05	1.44±0.11
L5	9.7±0.2	0.51±0.01	3.12±0.04	1.33±0.05

Table 2. Particle size, apparent amylose content, and digestibility of different WMSs.

Samples	D_{50} μm	AAC %	RDS %	SDS %	RS %
L1	12.2±0.0b	12.5±0.2a	37.4±1.5c	42.5±1.3a	20.1±0.2a
L2	12.4±0.1b	3.1±1.1c	49.2±0.9b	35.9±1.7b	15.0±0.8b
L3	11.6±0.1c	4.9±0.2b	38.4±0.6c	43.1±0.7a	16.9±1.0b
L4	13.3±0.6a	2.2±0.0c	45.9±3.0b	41.4±3.7a	12.7±0.7c
L5	12.1±0.0bc	1.8±0.1c	59.2±1.0a	31.1±2.0b	9.7±1.1d

Values followed by the different letter within a row differ significantly ($p < 0.05$). Values are presented as means ± SD (standard deviation). D_{50}, median diameter with half of granules above and half below this diameter; AAC, apparent amylose content; RDS, rapidly digestible starch; SDS, slowly digestible starch; RS, resistant starch.

Table 3. Molecular mass (M_w), R_g and its molecular mass distribution of different WMSs.

Samples	M_w (g/moL)	R_g (nm)	Molar mass distribution (%)				
			$< 5\times10^6$	5×10^6–1×10^7	1×10^7–2×10^7	2×10^7–3×10^7	$>3\times10^7$
L1	3.40×10^6 (2%)	121 (1%)	87.33	12.67	0	0	0
L2	8.21×10^6 (1%)	103 (1%)	16.53	63.65	19.82	0	0
L3	1.19×10^7 (1%)	111 (1%)	0	36.39	60.79	1.33	1.49
L4	2.23×10^7 (1%)	132 (1%)	0	0	23.49	67.88	8.63
L5	5.22×10^7 (1%)	134 (1%)	0	0	0	0	100

Table 4. Chain length distribution (%) of amylopectin of different WMSs.

Sample	f_a (DP 6–12)	f_{b1} (DP 13–24)	f_{b2} (DP 25–36)	f_{b3} (DP > 36)
L1	21.5±0.2a	43.2±0.1a	17.4±0.1d	17.9±0.4b
L2	20.9±0.1a	41.1±0.0b	18.5±0.0ab	19.6±0.0a
L3	20.8±1.3a	41.6±0.5b	18.0±0.2c	19.6±0.7a
L4	20.4±0.1a	41.7±0.1b	18.3±0.0b	19.7±0.2a
L5	20.6±0.2a	41.2±0.3b	18.7±0.1a	19.6±0.4a

Values followed by the different letter within a row differ significantly ($p < 0.05$). Values are presented as means ± SD (standard deviation).

Table 5. XRD, NMR and ATR-FTIR parameters of different WMSs.

Samples	RC %	SH %	DH %	AS %	$R_{1045/1022}$
L1	35.2±0.1d	3.31±0.08a	34.9±0.3a	61.8±0.3b	0.713±0.003a
L2	37.6±0.1c	1.63±0.01c	30.7±1.2c	67.7±1.2a	0.572±0.010b
L3	37.5±0.1c	1.97±0.01b	32.2±0.4bc	65.9±0.4a	0.604±0.033b
L4	38.2±0.1b	1.07±0.24d	32.0±0.9bc	66.9±1.1a	0.569±0.007b
L5	38.9±0.1a	0.00±0.00e	33.0±0.0b	67.0±0.0a	0.566±0.005b

Values followed by the different letter within a row differ significantly ($P < 0.05$). Values are presented as means ± SD (standard deviation). RC, relative crystallinity; DH, double helix; SH, single helix; AS, amorphous starch.

Table 6. SAXS parameters of different samples.

Samples	q_{peak} (nm^{-1})	D (Å)
L1	0.693	90.6
L2	0.700	89.8
L3	0.707	88.9
L4	0.700	89.8
L5	0.713	88.1

Table 7. Correlation analysis between the multi-scale structure and digestibility of waxy maize starch.

	RDS	SDS	RS
AAC	−0.696*	0.508	0.872**
D_{50}	0.212	−0.035	−0.299
f_a	−0.366	0.236	0.642*
f_{b1}	−0.672	0.543	0.746*
f_{b2}	0.862**	−0.749	−0.903
f_{b3}	0.470	−0.300	−0.741*
M_w	0.845**	−0.715*	−0.881**
R_g	0.378	−0.199	−0.510
q_{peak}	0.669*	−0.594	−0.742*
D	−0.666*	0.591	0.742*
D_m	−0.911**	0.730*	0.982**
SH	−0.887**	0.723*	0.974**
DH	−0.303	0.234	0.400
AS	0.647*	−0.518	−0.755*
$R_{1045/1022}$	−0.678*	0.501	0.803**
RC	0.772**	−0.590	−0.931**

** Correlation is significant at the 0.01 level (2-tailed). * Correlation is significant at the 0.05 level (2-tailed). AAC, apparent amylose content; D_{50}, median diameter with half of granules above and half below this diameter; q, position of scattering peak; D, average thickness of starch semi-crystalline lamellae; D_m, mass fractal dimension; RC, relative crystallinity; $R_{1045/1013}$, relative absorbance at 1045/1022; DH, double helix: SH, single helix; AS, amorphous starch; M_w, weight-average molecular weight; R_g, mean square radius of gyration; f_a, DP 6–12; f_{b1}, DP 13–24; f_{b2}, DP 25–36; f_{b3}, DP > 36.

Figure captions

Fig. 1. Granule size distributions of different WMSs.

Fig. 2. SEM images of different WMSs.

Fig. 3. 13C NMR spectra of different WMSs.

Fig. 4. XRD patterns of different WMSs.

Fig. 5. ATR-FTIR spectra of different WMSs.

Fig. 6. Double logarithmic SAXS patterns of different WMSs.

Figures

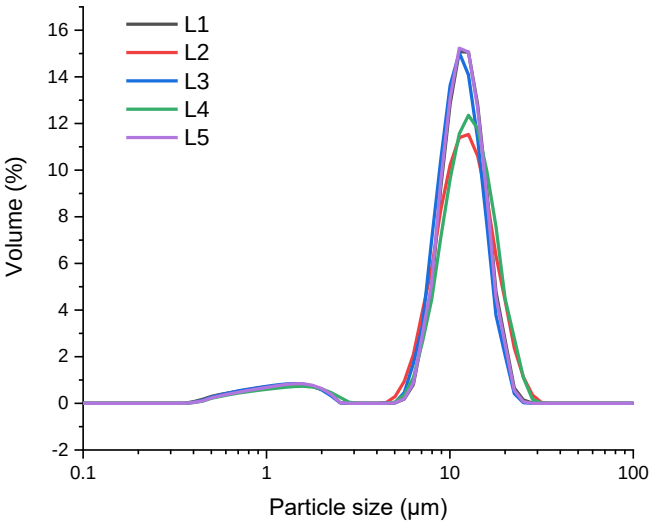

International Journal of Biological Macromolecules – Xu et al. – Fig. 1

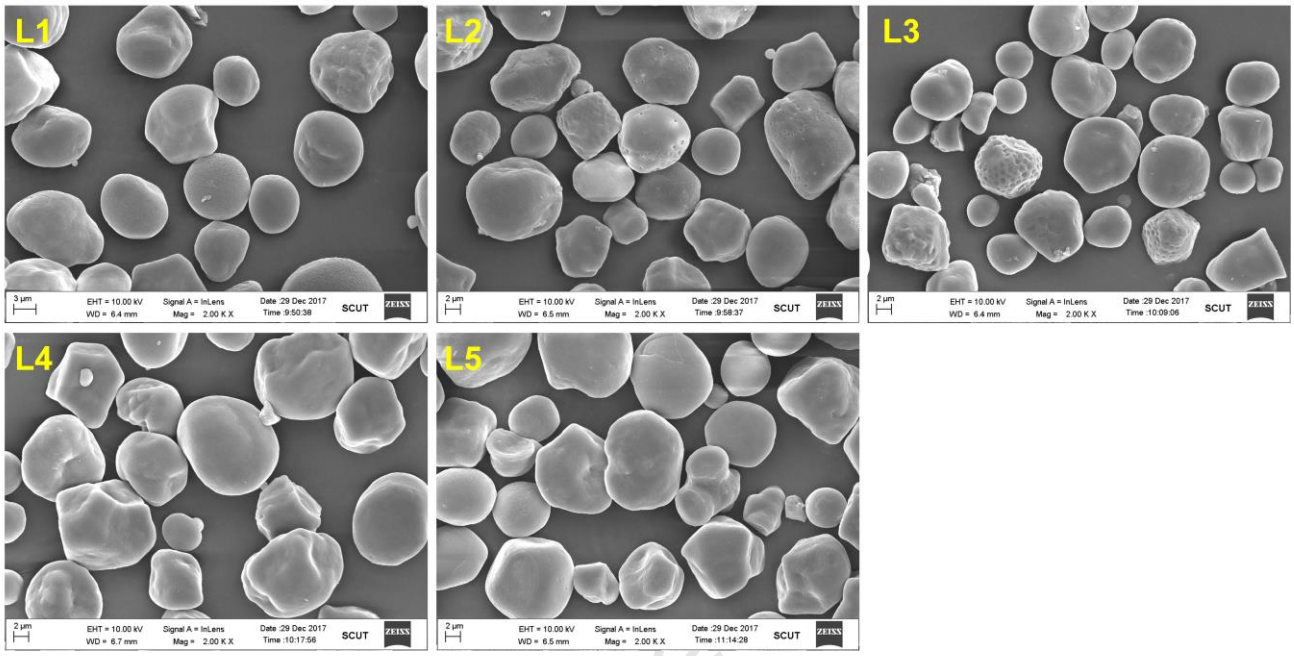

International Journal of Biological Macromolecules – Xu et al. – Fig. 2

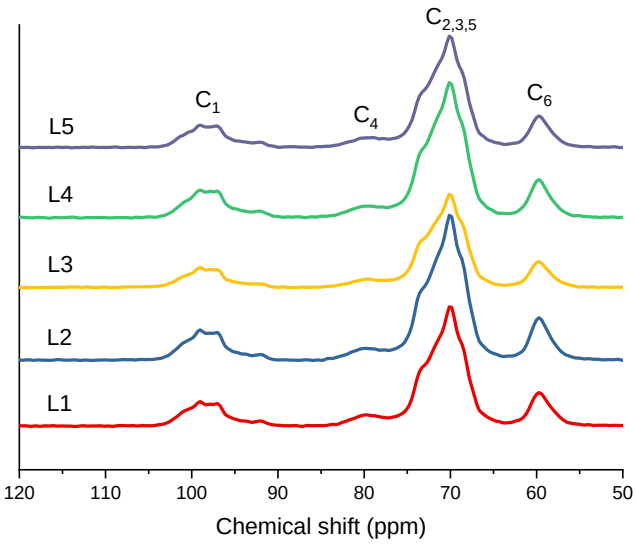

International Journal of Biological Macromolecules – Xu et al. – Fig. 3

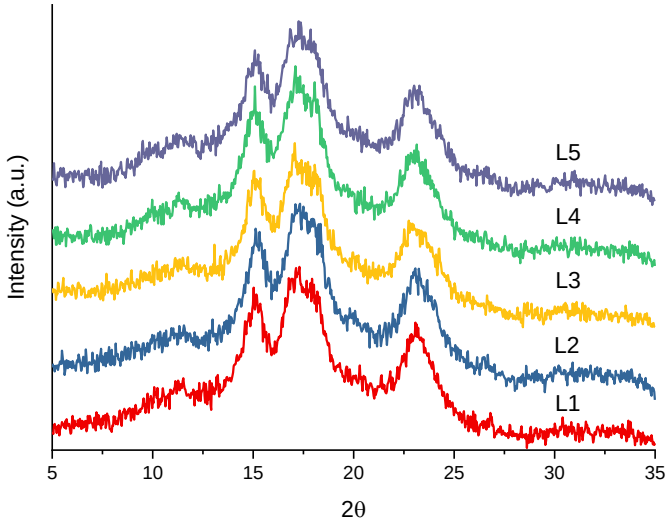

International Journal of Biological Macromolecules – Xu et al. – Fig. 4

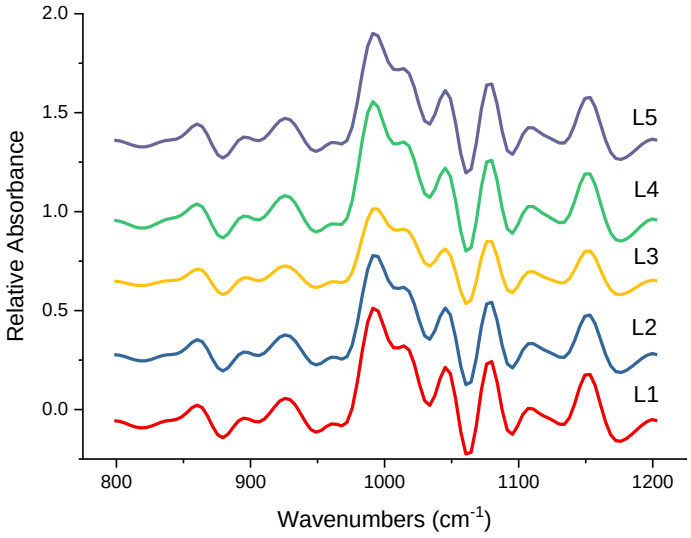

International Journal of Biological Macromolecules – Xu et al. – Fig. 5

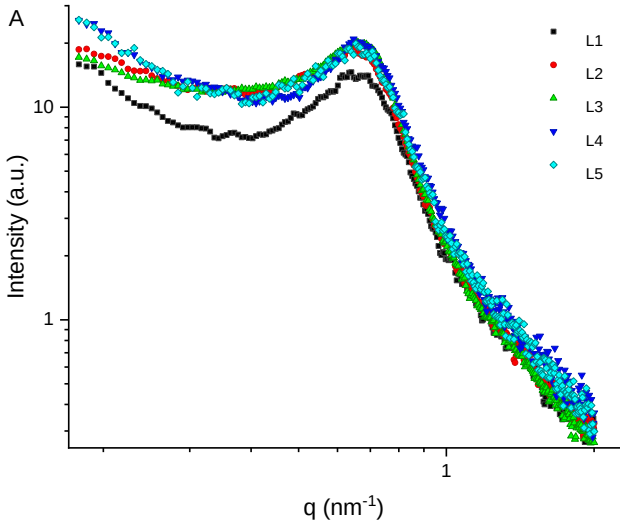

International Journal of Biological Macromolecules – Xu et al. – Fig. 6

CRediT author statement:

Jinchuan Xu: Methodology, Validation, Formal analysis, Investigation, Data Curation, Writing - Original Draft, Visualization. **Ling Chen:** Conceptualization, Methodology, Resources, Supervision, Project administration, Funding acquisition. **Xinbo Guo:** Conceptualization, Methodology, Resources. **Yi Liang:** Resources. **Fengwei Xie:** Methodology, Resources, Writing - Review & Editing, Visualization, Supervision, Funding acquisition.

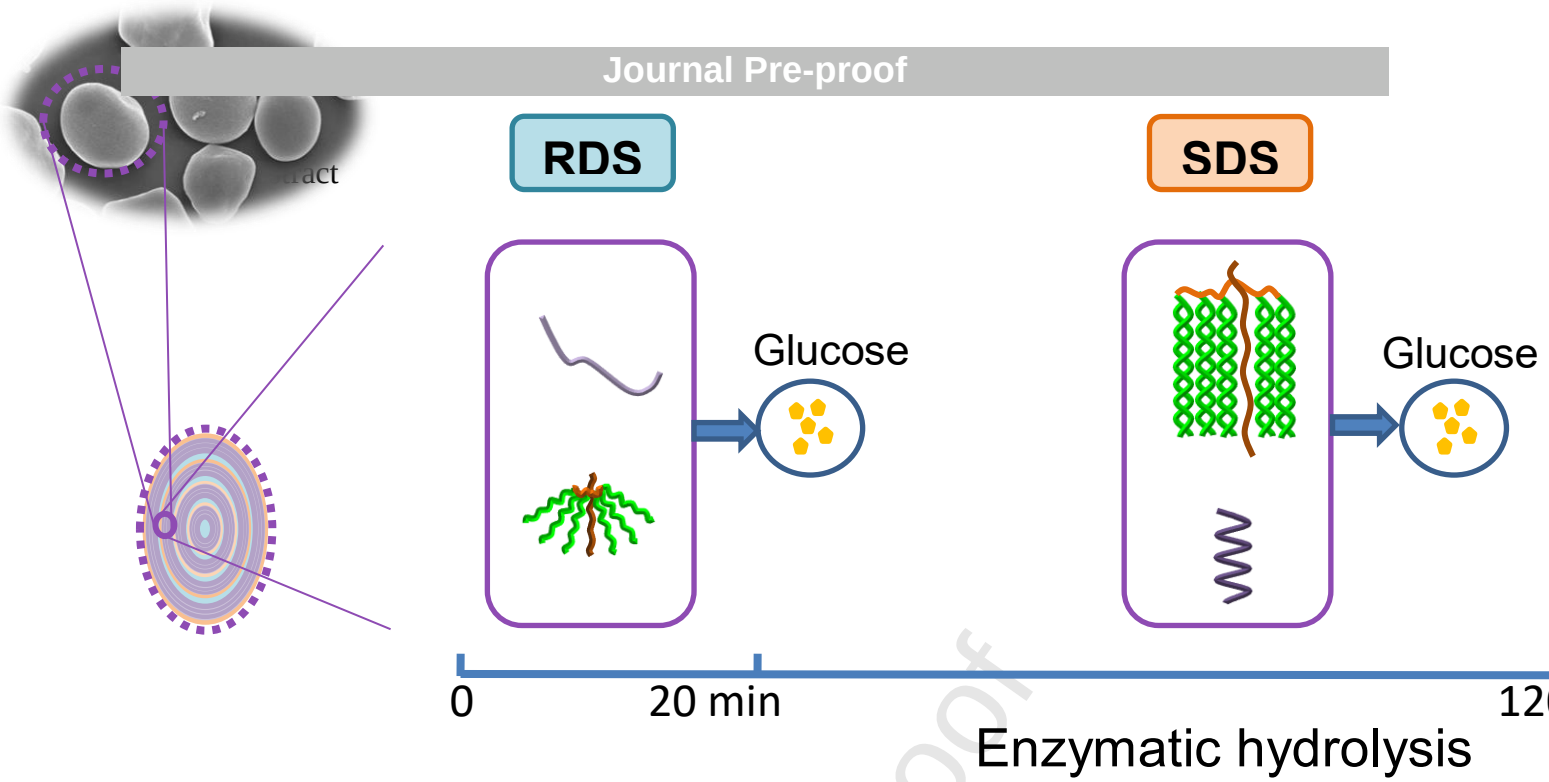

Highlights:

- ✓ Different waxy maize starches (WMSs) show varied structure and digestibility
- ✓ The digestibility strongly correlates with the multiscale structure of WMSs
- ✓ The surface porosity of WMS granules facilitates their digestibility
- ✓ Single helices and surface short-range ordered structures give resistant starch
- ✓ The quality of crystallites and the chain length determine the starch resistance